MICROBIOLOGY

Down-regulation of the bacterial protein biosynthesis machinery in response to weeks, years, and decades of soil warming

Andrea Söllinger[1]*, Joana Séneca[2], Mathilde Borg Dahl[3], Liabo L. Motleleng[1], Judith Prommer[2], Erik Verbruggen[4], Bjarni D. Sigurdsson[5], Ivan Janssens[4], Josep Peñuelas[6,7], Tim Urich[3], Andreas Richter[2], Alexander T. Tveit[1]*

How soil microorganisms respond to global warming is key to infer future soil-climate feedbacks, yet poorly understood. Here, we applied metatranscriptomics to investigate microbial physiological responses to medium-term (8 years) and long-term (>50 years) subarctic grassland soil warming of +6°C. Besides indications for a community-wide up-regulation of central metabolic pathways and cell replication, we observed a down-regulation of the bacterial protein biosynthesis machinery in the warmed soils, coinciding with a lower microbial biomass, RNA, and soil substrate content. We conclude that permanently accelerated reaction rates at higher temperatures and reduced substrate concentrations result in cellular reduction of ribosomes, the macromolecular complexes carrying out protein biosynthesis. Later efforts to test this, including a short-term warming experiment (6 weeks, +6°C), further supported our conclusion. Down-regulating the protein biosynthesis machinery liberates energy and matter, allowing soil bacteria to maintain high metabolic activities and cell division rates even after decades of warming.

INTRODUCTION

Global temperatures and atmospheric carbon dioxide (CO_2) levels have increased steadily over the past 100 years (*1*, *2*). Feedbacks from the terrestrial carbon (C) cycle to the climate system represent a major uncertainty in the prediction of future temperatures (*3*). Soil microorganisms, including bacteria, archaea, fungi, and microbial eukaryotes, play a key role in the terrestrial C cycle by being responsible for the turnover of soil organic matter (SOM) and the subsequent release of CO_2 from soils to the atmosphere (*2*). Higher temperatures commonly lead to higher microbial activities, so global warming should accelerate the decomposition of SOM to CO_2 (*4*). On the other hand, SOM consists largely of microbial necromass and warming may stimulate microbial growth and thus necromass production (*5*, *6*), promoting SOM formation. Whether soils will ultimately act as C sinks or sources thus depends on how microorganisms respond to long-term warming. Nevertheless, microbial responses to global warming are currently poorly represented in Earth system models (*7*), which can, to some extent, be attributed to the challenges associated with studying and quantifying microbial responses to environmental change in complex soil environments (*4*).

Microbial responses to long-term soil warming may include (i) quantitative and compositional changes of microbial communities, (ii) physiological adjustments of individual microorganisms, including changes in growth and resource use, via transcriptional and translational regulation, (iii) shifts in microbial interactions and emergent properties of the community, and (iv) microbial adaptations by genomic rearrangements and evolutionary changes of the genetic code.

In one of the few truly long-term warming studies (Harvard Forest Warming Experiment: 26 years, +5°C, midlatitude forest soil) (*8*), the observed warming effects on the microbial community included a decrease in fungal biomarkers and abundance, a decrease in microbial biomass, a community shift toward Gram-positive bacteria, and an increase in bacterial evenness and abundance of bacteria with low copy numbers of ribosomal RNA (rRNA) operons. A meta-analysis of 25 in situ soil warming experiments (1 to 15 years, +0.5° to 5.5°C, various soil ecosystems) found initial increases in soil respiration (46 ± 8%) due to warming followed by significant decreases over time (*9*). However, less than half of the studies estimated microbial biomass, and two-thirds of the studies that quantified changes reported decreases in microbial biomass with warming. Increased rates of SOM degradation and soil respiration followed by a return to prewarming rates within a few years were repeatedly observed (*10*). This pattern is often explained by an "acclimation of soil respiration," a shift in the response of respiration to ongoing warming that leads to different sensitivities of soil respiration to temperature [(*11*, *12*) and references therein]. Alternatively, a return to prewarming states can be explained by the depletion of easily degradable substrates (*10*, *13*).

It has recently been shown that natural geothermal activity can enable the study of soil warming on decadal time scales (*14*, *15*). We here make use of the longest lasting in situ soil warming experiment worldwide, ForHot, in which a subarctic grassland site has been exposed to natural geothermal soil warming for decades (>50 years) (*14*). More recent soil temperature gradients emerged nearby after an earthquake in 2008. The effects of short- to medium-term and long-term soil warming on abiotic and biotic properties and processes at these sites have been described in a range of publications. For example, Walker *et al.* (*16*), Marañón-Jiménez *et al.* (*17*, *18*), and Poeplau *et al.* (*19*) identified considerable soil environmental changes in the warmed grassland plots, including reductions in topsoil C and nitrogen (N) pools by about 40% and decreased soil aggregation. These changes were accompanied by lower soil microbial

[1]Department of Arctic and Marine Biology, UiT The Arctic University of Norway, Tromsø, Norway. [2]Centre for Microbiology and Environmental Systems Science, University of Vienna, Vienna, Austria. [3]Institute of Microbiology, University of Greifswald, Greifswald, Germany. [4]PLECO, University of Antwerp, Antwerp, Belgium. [5]Agricultural University of Iceland, Borgarnes, Iceland. [6]CSIC, Global Ecology Unit CREAF-CSIC-UAB, Barcelona, Spain. [7]CREAF, Barcelona, Spain.
*Corresponding author. Email: andrea.soellinger@uit.no (A.S.); alexander.t.tveit@uit.no (A.T.T.)

biomass but higher growth and respiration rates per unit of microbial biomass (16), the latter contradicting the concept of a physiological acclimation of microorganisms (16). Recently, a meta-analysis on 128 measured variables at these sites, including a broad variety of biotic and abiotic soil properties, pools, and processes, was published, reporting a systemic overreaction to 5 to 8 years versus decades of warming (15). The authors proposed that an initial acceleration of biotic activity due to warming led to rapid decreases in C, N, and P pools within the first years after the onset of warming, followed by a decrease of microbial and fungal biomass and system stabilization within decades. However, details of underlying microbial responses influencing the ecosystem-scaled responses remained largely unexplored.

Here, we aimed at providing the first in-depth functional analysis of soil microbial responses to warming using a metatranscriptomics approach, i.e., high-throughput shotgun sequencing of total RNA. In contrast to DNA-based methods (e.g., metagenomics or amplicon sequencing), which can only show genetic potential and are often restricted to specific microbial groups, metatranscriptomics allows the comprehensive study of the soil microbiome, i.e., the entire active soil microbial community (bacteria, archaea, eukaryotes, and viruses) and their functions, by studying expressed genes (mRNA and rRNA) (20). In this study, we analyzed 16 soil microbiomes. In situ microbial gene expression profiles of medium-term warmed soils (MTW) exposed to +6°C for 8 years and long-term warmed soils (LTW) exposed to +6°C above ambient (E_T) for >50 years were compared to ambient controls (A_T). In addition, we measured physicochemical soil properties [e.g., dissolved and total soil C, N, and phosphorus (P) concentrations] and estimated microbial biomass. Our main objective was to elucidate if and how soil microorganisms alter their cellular activities and functions in response to warming and reveal if previous observations of higher biomass-specific microbial growth and respiration rates are related to changes in microbial gene expression.

RESULTS AND DISCUSSION

Warming effects on soil physicochemical and biological properties

We analyzed subarctic grassland soil samples from eight stable natural soil temperature gradients, established and maintained by geothermal activity, located in the same landscape at two adjacent sites being subject to sustained soil warming for years (8 years; MTW, medium-term warming site; four gradients) and decades (>50 years; LTW, long-term warming site; four gradients; Fig. 1A), respectively. The analyzed samples comprised two distinct soil temperature regimes (A_T, ambient soil temperatures and E_T, +6°C above ambient soil temperatures). To evaluate sample selection and characterize the individual sample groups, we analyzed soil physicochemical and biological properties (table S1). On average, total C, N, and P (C_{tot}, N_{tot}, and P_{tot}), dissolved organic C and P (DOC and DOP), and microbial C, N, and P (C_{MO}, N_{MO}, and P_{MO}), as well as RNA and water content were higher in the nonwarmed soils (A_T) than in E_T (Fig. 1B). Dissolved organic N (DON) and DNA content varied considerably between MTW and LTW, resulting in a lack of consistent differences between A_T and E_T for these variables. The pH was slightly higher in E_T. These properties were individually tested for significant differences between defined groups (Fig. 1B, right, and table S2). Significant differences were mainly observed between the two temperature groups A_T and E_T. While C_{tot}, N_{tot}, and P_{tot} did not differ significantly between A_T and E_T (P_{adj} = 0.093 – 0.096), pH, DOC, and DOP, as well as most biological properties (C_{MO}, N_{MO}, P_{MO}, and RNA content) did. Besides DON, no significant differences between the two nonwarmed control groups (MTW-A_T and LTW-A_T) were observed (Fig. 1B). These results largely mirror previous studies conducted at the same sites that also report lower substrate concentrations and microbial biomass contents in the warmed soils (15–18), indicating high reproducibility and suitability of the experimental sites for a comparative analysis of medium- and long-term warming effects.
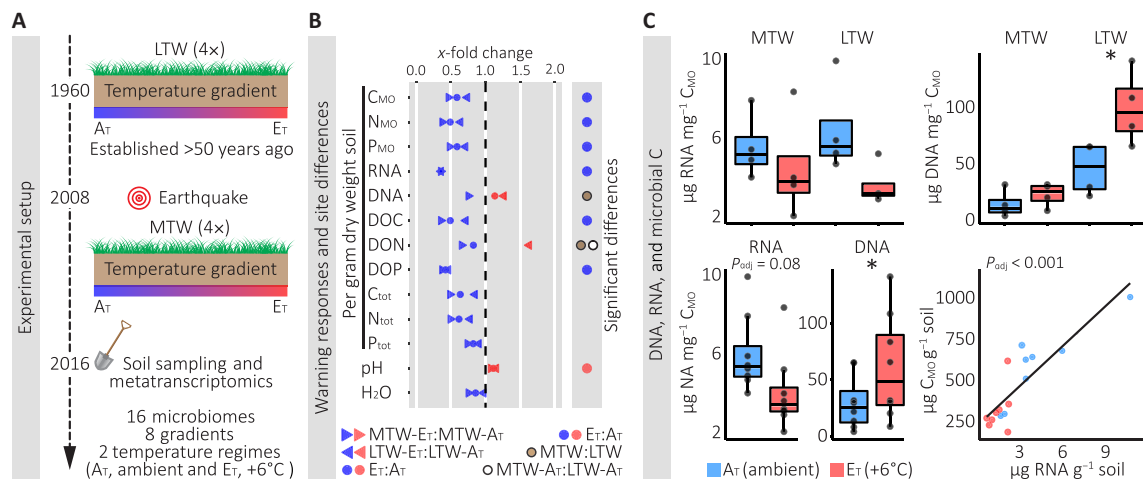
Fig. 1. Grassland soil samples and differences in physicochemical and biological properties. (A) Schematic overview of the ForHot experimental warming sites and analyzed samples (see Materials and Methods for more details). **(B)** Average x-fold change of soil physicochemical and biological properties in response to warming (see table S1 for absolute values). Values <1 represent measures that are lower in the warmed soils (i.e., higher in A_T, highlighted in blue), and values >1 represent measures that are higher in the warmed soils (highlighted in red). Triangles and dots (left) indicate site and temperature contrast (average x-fold change of MTW-E_T versus MTW-A_T, LTW-E_T versus LTW-A_T, and E_T versus A_T). Dots (right) indicate site and temperature contrast with significant differences in the respectively aligned physicochemical and biological properties (two-way ANOVAs on each individual property, TukeyHSD test to correct for multiple testing; see table S2 for the full statistical analysis and exact P values). **(C)** Nucleic acid (DNA and RNA) content per unit of microbial C (boxplots) and correlation between microbial C (C_{MO}) and RNA content per gram dry weight soil (scatterplot). See tables S2 and S3 for the full statistical analysis and exact P values (*P_{adj} < 0.05).

Total RNA and DNA content per unit of soil ranged from 0.71 to 10.71 µg g^{-1} dry weight soil and 2.23 to 70.45 µg g^{-1} dry weight soil, respectively. In addition to the lower RNA contents in the warmed plots (Fig. 1B) and a strong linear correlation between microbial biomass (using microbial C as proxy) and RNA per gram dry weight soil (Fig. 1C, scatterplot, and table S3), we observed a trend toward lower RNA content per unit of microbial biomass in the warmed soils (P_{adj} = 0.083). This was contrasted by a significantly higher DNA content per unit of microbial biomass (Fig. 1C, boxplots).

Together, our observations are in line with previous studies that characterized these warmed plots as significantly divergent from their nonwarmed counterparts (15–19). The new observations also support the proposition that an initial acceleration of biotic activity due to warming leads to decreases in C, N, and P pools within the first years after the onset of warming, followed by a decrease of microbial biomass (15). Warming also affected the ratio between nucleic acids and microbial biomass, an observation that, to our knowledge, was not made previously.

Warming effects on microbial gene expression

Illumina paired-end sequencing of total RNA from 16 soil samples produced an average of 6.69×10^6 mRNA reads per sample (table S4). Bacteria dominated the mRNA read pools (93.36 to 98.52%), followed by Eukaryota (1.28 to 6.45%), Archaea (0.5 to 1.6‰), and viruses (0.2 to 1.9‰). An average of 2.66×10^6 mRNA reads per sample was assigned to a molecular function (KO number) defined in the Kyoto Encyclopedia of Genes and Genomes (KEGG) Orthology database (table S4) (21). These reads were also dominated by Bacteria, accounting for 90.82 to 98.47% of the functionally annotated mRNA reads (see table S5 for a detailed comparison). We further analyzed all functionally annotated mRNA reads assigned to a KEGG metabolic pathway or functional complex. Rarefied abundance counts (table S6) indicate no significant effect of warming on functional richness (fig. S1 and table S7), while a permutational multivariate analysis of variance (PERMANOVA) analysis revealed a significant effect of warming on the composition of expressed KOs assigned to a KEGG metabolic pathway or functional complex (fig. S2 and table S8). To identify the nature of this functional response, we explored in more detail the functional assignments to KEGG categories and performed a differential gene expression (DGE) analysis. KEGG offers a hierarchical structure with four layers, KEGG1 (broad functional categories), KEGG2 (functional subcategories), KEGG3 (functional pathways and complexes), and KO (molecular functions, i.e., orthologous genes encoding proteins, enzymes, and enzyme subunits). In total, 3164 unique KOs assigned to a KEGG metabolic pathway or functional complex were detected in the metatranscriptomes. Of all functionally annotated mRNA reads, 78.9%, represented by 2732 KOs, were assigned to only one KEGG1 category (fig. S3), while the remaining mRNA reads were assigned to two or more KEGG1 categories. To avoid redundancy, we next explored the reads assigned to a single KEGG1 category and corresponding KEGG2 subcategories. Their distribution across the soil temperature groups led to four major observations (fig. S3): (i) Higher relative gene expression levels for major subcategories such as *Carbohydrate metabolism*, *Amino acid metabolism*, and *Lipid metabolism* in the warmed soils (KEGG1: *Metabolism*). (ii) Lower relative gene expression levels for *Energy metabolism* in the warmed soils (KEGG1: *Metabolism*). (iii) Lower relative gene expression levels for subcategories associated with protein biosynthesis, i.e., *Translation*,

Folding, *sorting & degradation*, and *Transcription*, in the warmed soils (KEGG1: *Genetic information processing*). (iv) Higher relative gene expression levels for *Replication & repair* in the warmed soils, albeit most pronounced in MTW-E$_T$ (KEGG1: *Genetic information processing*). Only within the KEGG1 category, *Metabolism*, a substantial fraction of the reads was assigned to two or more KEGG2 categories. Within the other KEGG1 categories, the fractions of ambiguous assignments were <1% of all KEGG2 assignments (table S9). The very same observations (i.e., i to iv) were made if all ambiguous assignments were included (fig. S4).

These initial findings pointed toward substantial overall changes in the most basic cellular functions such as protein biosynthesis, replication, energy conservation, and central metabolism. Next, we used an abundance pattern filter (see Materials and Methods) to identify KEGG3 pathways and functional complexes exhibiting putative warming-induced differential expression. More than 40% of all mRNA reads assigned to a KEGG metabolic pathway or functional complex were associated with KEGG3 categories that exhibited warming-induced differential abundance patterns (fig. S6 and table S10). Out of 56 KEGG3 categories with a visually distinct pattern, 13 showed lower relative gene expression levels in E$_T$ than A$_T$, while 43 KEGG3 categories showed higher relative gene expression levels in E$_T$ than A$_T$. The comparatively high relative abundances of eukaryotic mRNA reads in the LTW-A$_T$ samples (4.7% ± 1.8 SD) compared to MTW-A$_T$, MTW-E$_T$, and LTW-E$_T$ (1.5% ± 0.6 SD) may skew or mask biologically and ecologically relevant changes. Thus, we complemented the abundance pattern analysis with a DGE analysis on the KO level (orthologous genes), excluding eukaryotic assignments. A total of 787 KOs were included in the DGE analysis (see Materials and Methods), out of which 66 KOs (i.e., 8.4%) were differentially expressed [false discovery rate (FDR) < 0.05] when comparing all A$_T$ with all E$_T$ soils (table S11). Comparing gene expression profiles of MTW-A$_T$ and LTW-A$_T$ revealed no significant differences between the two nonwarmed control groups (table S11). We then assigned the differentially expressed KOs to the hierarchical KEGG structure (table S12). The majority of the differentially expressed KOs fell within KEGG3 categories associated with protein biosynthesis, i.e., *Ribosome*, *Protein export*, *RNA polymerase*, and *RNA degradation*. In addition, several KOs assigned to these functional categories with an FDR between 0.05 and 0.1 shared the same expression pattern. The overall expression of genes for all of these functions was lower in the warmed soils (fig. S7), indicating a down-regulation of the protein biosynthesis machinery in warmed soils. Furthermore, several differentially expressed KOs were assigned to the energy metabolism KEGG3 category *Oxidative phosphorylation*, the lower overall expression of these genes in the warmed soils (fig. S7) indicating a down-regulation of membrane-bound energy-harvesting complexes. The majority of the remaining differentially expressed KOs were associated with one or more pathways of central carbohydrate metabolism, nucleotide metabolism, and amino acid metabolism. Lists of all differentially expressed KOs and KOs with an FDR between 0.05 and 0.1 are provided as supplementary tables (tables S13 to S15).

Down-regulated enzymes and enzyme complexes
The protein biosynthesis machinery

Because of the high number of differentially expressed KOs encoding enzymes involved in protein biosynthesis (fig. S7), we decided to analyze this aspect of cellular metabolism in more detail. Our

analysis included (i) the bacterial DNA-directed RNA polymerase, responsible for the transcription of DNA into rRNA, mRNA, and small noncoding RNAs, (ii) the bacterial ribosome, consisting of ribosomal proteins and rRNA and the site of protein synthesis (translation of mRNA into peptides), (iii) bacterial RNA degradosomes, responsible for the degradation and recycling of RNAs, (iv) bacterial protein folding complexes, responsible for the proper folding of peptides into mature proteins, and (v) the bacterial Sec-dependent pathway of posttranslational translocation of proteins across membranes (Fig. 2A, drawings). The relative abundances of mRNA reads encoding RNA polymerase subunits, ribosomal proteins, GroEL and DnaK (protein folding), and Sec translocase subunits (protein export) were consistently lower in the warmed soils (Fig. 2A, boxplots). For all these enzyme complexes, we found a substantial fraction of KOs with significantly lower relative expression levels in the warmed soils, the pattern being largely consistent between MTW and LTW

(Fig. 2A, table, and table S16). KOs encoding ribosomal proteins accounted for most of the differentially expressed KOs, with significantly lower relative expression levels in the warmed soils (overall 19 KOs). Within MTW, 22 ribosomal proteins showed significantly lower relative KO expression levels in the warmed soils, supported by eight ribosomal proteins with lower but not significant relative KO expression levels in the warmed soils (FDR, 0.05 to 0.1). In LTW, we observed significantly lower relative KO expression levels in the warmed soils for seven ribosomal proteins. Ten ribosomal protein–encoding genes with lower, but not significantly different, relative KO expression levels in the warmed soils supported this observation (FDR, 0.05 to 0.1; table S16). Two ribosomal proteins showed significantly higher relative expression levels in the warmed soils of LTW, indicating that not all ribosomal proteins are regulated by the same feedback mechanisms (22). The expression of Sec subunits (protein export) showed highly consistent temperature responses in
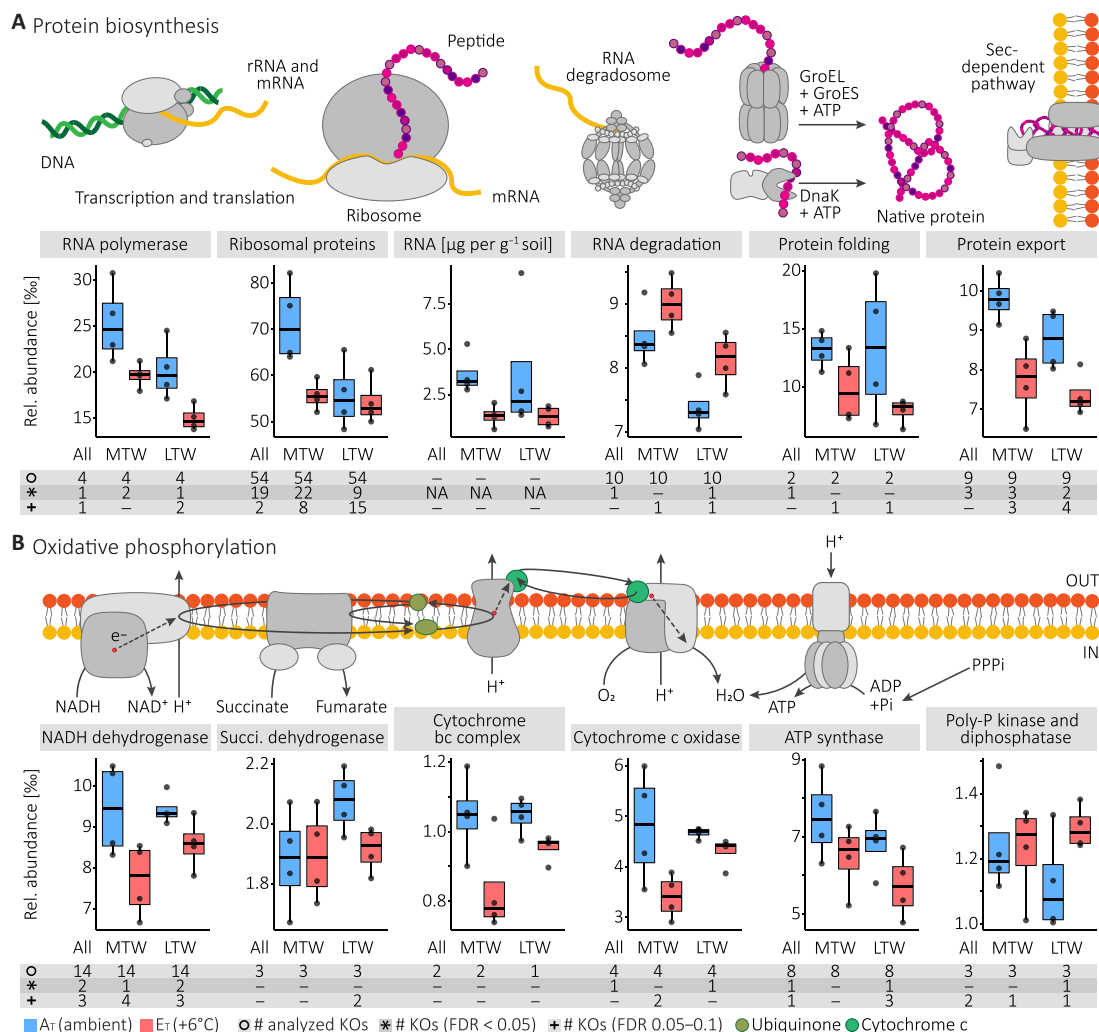

Fig. 2. Enzymes and enzyme complexes involved in protein biosynthesis and oxidative phosphorylation. (**A**) Relative mRNA read abundances of protein biosynthesis complexes in the MTW-A_T, MTW-E_T, LTW-A_T, and LTW-E_T metatranscriptomes (boxplots) and DGE analysis results on associated KOs (table). (**B**) Relative mRNA read abundances of complexes involved in membrane-bound electron transport and ATP synthesis (oxidative phosphorylation) in the MTW-A_T, MTW-E_T, LTW-A_T, and LTW-E_T metatranscriptomes (boxplots) and DGE analysis results on associated KOs (table). Schematic representations of the enzymes and enzyme complexes are provided above the boxplots and are based on the KEGG pathway drawings. Membrane-bound complexes are embedded in a lipid bilayer. See table S16 for relative abundances of all individual KOs summarized in the boxplots and details on the DGE analysis.

MTW (table S16). While less clear in LTW, the summarized mean relative mRNA abundances were overall lower in the warmed soils (Fig. 2A, Protein export—boxplot). A contrasting temperature response was shown for RNA degradosome subunits, with overall higher, but not significantly different, expression in the warmed soils relative to the ambient soils (Fig. 2A). Together, our results suggest that the entire protein biosynthesis machinery, including enzyme complexes involved in transcription, translation, and protein processing, may be down-regulated in the microbiomes subject to soil warming of +6°C above ambient temperatures, irrespective of the duration of warming (8 years versus >50 years). Notably, the lower relative abundances of mRNA reads encoding ribosomal proteins suggest a down-regulation of ribosome synthesis in the warmed soils. This was supported by the lower total RNA content per unit of soil (Fig. 2A, RNA—boxplots) and total RNA content per unit of microbial C (Fig. 1C) in both MTW and LTW.

Energy metabolism

We observed lower expression of KOs associated with the *Energy metabolism* subcategory *Oxidative phosphorylation* in the warmed soils (fig. S7). Oxidative phosphorylation is the final step in aerobic respiration (Fig. 2B, drawings). Electrons harvested from the oxidation of carbohydrates are transferred via a membrane-bound electron transport chain, O_2 acts as terminal electron acceptor, and the generated proton-motive force is used by the adenosine triphosphate (ATP) synthase to phosphorylate adenosine diphosphate (ADP) and produce ATP, the major energy currency of all cells. Although respiratory electron transport chains vary among bacteria (*23*), we observed lower mean relative abundances of multiple common complexes including ATP synthase in the warmed soils (Fig. 2B, boxplots). Of all investigated membrane-bound complexes, only succinate dehydrogenase, and only in MTW, did not exhibit a warming-dependent expression pattern. However, succinate dehydrogenase represents a non–pathway-specific enzyme (*21*), offering a potential explanation. Despite few genes being significantly differentially expressed (Fig. 2B, table), the large number of genes encoding metabolically connected membrane-bound enzyme complexes displaying a lower mean relative expression level in the warmed soils suggests that down-regulation of the oxidative phosphorylation complexes may be a microbial response to soil warming.

Up-regulated enzymes and enzyme complexes
Central (carbohydrate) metabolism

KEGG2 and KEGG3 categories with overall higher relative expression levels in the warmed soils were to a large extent observed within the KEGG1 category *Metabolism* (figs. S3, S6, and S7), prompting us to analyze community transcript profiles focusing on central (carbohydrate) metabolism (Fig. 3A). We observed only few differentially expressed KOs, but all had higher relative expression levels in the warmed soils. Individual KEGG metabolic pathway maps (*21*) reflecting KEGG3 categories (e.g., *Pyruvate metabolism*, *Glycolysis/Gluconeogenesis*, and *Methane metabolism*) overlap, and the few differentially expressed KOs mainly represent KOs assigned to several KEGG3 categories. Nevertheless, a few noteworthy observations were made (Fig. 3A).

Enzymatic reaction steps leading from pyruvate to *Fatty acid biosynthesis* via acetyl–coenzyme A (CoA) showed higher relative expression levels in the warmed soils, while steps leading from pyruvate to *Oxidative phosphorylation* showed the opposite trend, irrespective of the duration of warming (8 years versus >50 years)

(Fig. 3A). This matches our detailed analysis on *Fatty acid biosynthesis* (fig. S8) and *Oxidative phosphorylation* (Fig. 2B), as an up-regulation of fatty acid biosynthesis would require an increased flow of C from the central intermediates, acetyl-CoA, and pyruvate, while a down-regulation of *Oxidative phosphorylation* might be linked to a down-regulation of succinate supply. Some integral pathways exhibited inconsistent temperature responses. For example, the first steps in glycolysis (from α-D- and β-D-glucose to β-D-fructose-6P) showed higher relative expression levels in the warmed soils and include differentially expressed KOs (Fig. 3A). However, most subsequent steps did not reveal a clear temperature trend. A previous in situ study on samples from the same LTW plots, taken one summer earlier, reported significantly higher biomass-specific organic C uptake rates (mg C g^{-1} C_{MO} $hour^{-1}$) and higher biomass-specific respiration rates (mg C g^{-1} C_{MO} $hour^{-1}$) in the warmed soils (E_T, +6°C) compared to their ambient counterparts (*16*). However, unlike the very consistent patterns within protein biosynthesis described above, our more detailed investigation of central (carbohydrate) metabolism did not reveal sufficiently convincing patterns to conclude that a common microbial up-regulation of central (carbohydrate) metabolism is occurring due to soil warming, and ambiguous KOs complicate the interpretation. A recently published metatranscriptomics study investigating microbial functional responses to long-term forest soil warming (Harvard Forest Warming Experiment: 30 years, +5°C) suggested that warming might lead to increased abundances of enzymes related to polysaccharide and lipid metabolism and decomposition in forest soils, indicating possible differences in the microbial response to long-term warming in forest soils and grassland soils (*24*).

Cell replication

We observed higher relative expression levels for amino acid and nucleotide biosynthesis and metabolism (fig. S7), *Glycerolipid metabolism* (fig. S7), *Fatty acid biosynthesis* (fig. S8), and *Peptidoglycan biosynthesis* (fig. S6), important pathways in the production of major biomolecule building blocks and cell membrane and cell wall biosynthesis. Together, these results prompted us to have a closer look at cell replication (Fig. 3, B and C). Bacterial cell replication can be divided into two closely interacting cycles: (i) the DNA cycle, i.e., DNA replication and chromosome segregation, and (ii) the division cycle, i.e., cytokinesis and cell separation (*25*). FtsZ is a key enzyme and regulator of bacterial cell division, and an up-regulation of its synthesis has been shown to correlate with the formation of the Z-ring, a ring-like structure at the division site constricting during cell division (*25, 26*). We saw indications for higher average expression levels of DNA polymerase III subunits and DNA replication initiation factors (Fig. 3B) as well as higher average expression levels of FtsZ in the warmed soils (Fig. 3C), but these patterns were not significant. Cellular DNA content depends on the stage of growth, usually being higher in actively replicating cells (*27*). The total DNA content per unit of microbial C was significantly higher in the warmed soils (Fig. 1C), further indicating a higher relative abundance of cells being replicated in the warmed soils. This interpretation is strongly supported by a previous study reporting significantly higher biomass-specific microbial growth rates (mg C g^{-1} C_{MO} $hour^{-1}$; measured via DNA replication rates) in samples from the same LTW plots (E_T, +6°C) taken one summer earlier, compared to their ambient counterparts (*16*). However, extracellular or relic DNA stemming from dead microorganisms, which can represent up to 40% of prokaryotic and fungal DNA in soil (*28*), could
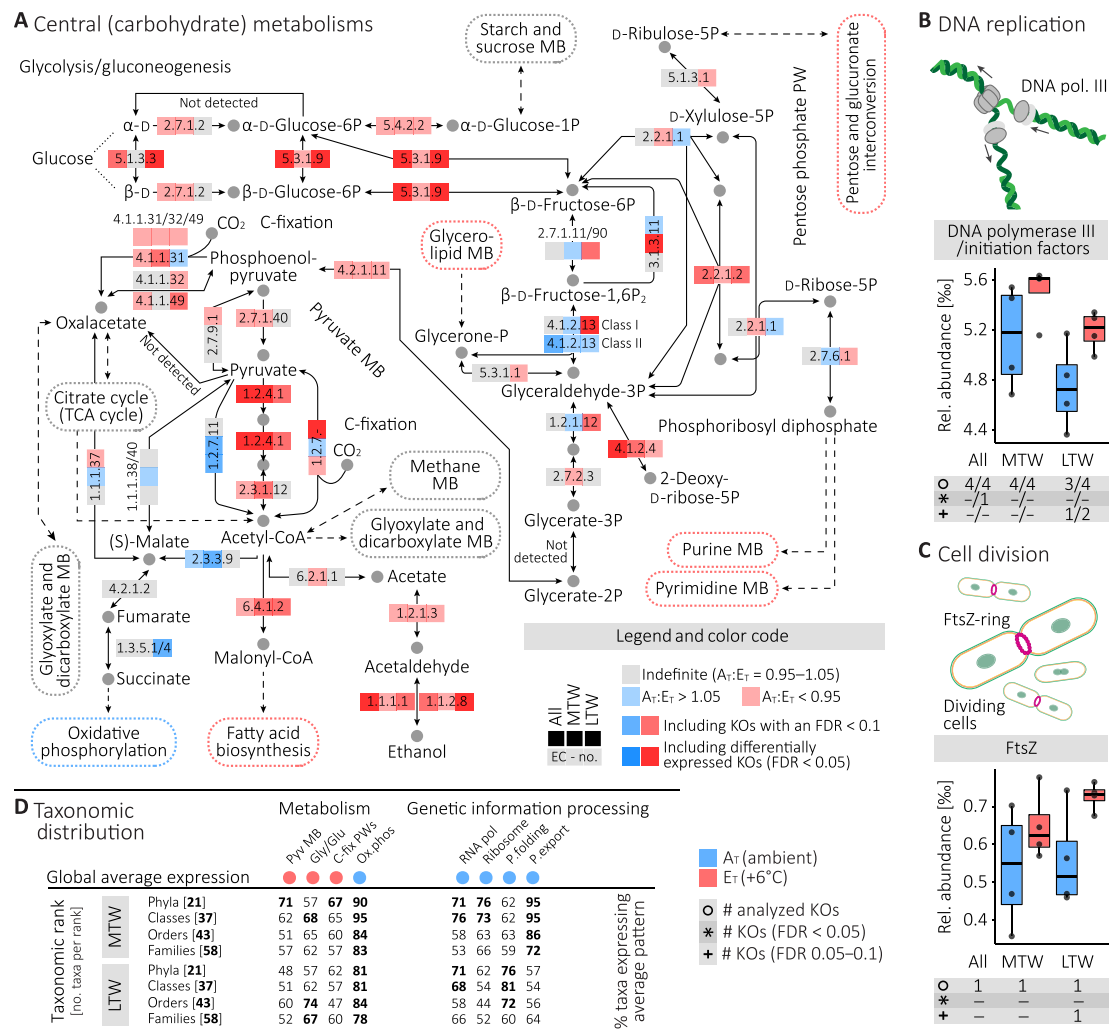
Fig. 3. Enzymes and enzyme complexes involved in central carbohydrate metabolism and cell replication and taxonomic distribution of overall expression patterns. (**A**) Metabolic pathway map focusing on carbohydrate metabolism, associated reactions, and relative mRNA read abundances assigned to these reactions. Reactions are represented by EC numbers (EC-no.) and derived from KEGG pathway drawings. Color code indicates mean relative expression levels (red, higher relative expression levels in E_T; blue, higher relative expression levels in A_T); intensities additionally reflect the presence of differentially expressed KOs and KOs with an FDR of 0.05 to 0.1. Bold fonts indicate Metabolism subcategories (KEGG3); dashed arrows indicate connections to subcategories for which no details are given; the color code (as above) of the frames around these categories indicates if the whole subcategory shows indications of a temperature-dependent response. See table S17 for details. (**B** and **C**) Cell replication. Relative mRNA read abundances of DNA polymerase III subunits, bacterial initiation factors (B) and FtsZ (C) in the metatranscriptomes (boxplots), and DGE analysis results on associated KOs (table; see table S16 for details). Schematic illustrations are provided above the boxplots. (**D**) Taxonomic distribution of observed overall expression patterns on abundant KEGG3 categories comprising genes encoding key functions in central carbohydrate metabolism with higher expression levels and genes encoding key functions in energy metabolism and protein biosynthesis with lower expression levels in the warmed soils, respectively. Pyv MB, pyruvate metabolism; Gly/Glu, glycolysis/gluconeogenesis; C-fix PWs, C fixation pathways in prokaryotes; Ox.phos, oxidative phosphorylation; RNA pol, RNA polymerase; P., protein. Bold numbers aligned to a KEGG3 category highlight taxonomic ranks in which the taxon-specific expression pattern of more than two-thirds of all included taxa (i.e., all taxa with a mean relative abundance of ≥1‰) reflected the global expression pattern of the respective KEGG3 category (see also fig. S11).

also have contributed to the higher DNA:biomass ratios in the warmed soils.

Decoupling of microbial community structure and functional temperature response

A simple explanation for changes in gene expression between ambient and warmed microbiomes could be a compositional change in the active microbial communities as a response to warming. Therefore, we analyzed the taxonomic composition of mRNA read pools in detail, combining diversity and variance analysis with abundance pattern and DGE analyses. An average of 6.02×10^6 mRNA reads per sample was taxonomically classified (table S4). As described above, mRNA read pools were largely dominated by Bacteria (93.36 to 98.52%; fig. S9 and table S5). Overall, more than 1000 different prokaryotic, eukaryotic, and viral families were detected in the metatranscriptomes (table S6). Mean family richness did not differ significantly between warmed soils and their ambient counterparts (table S7), albeit showing a trend toward a reduced richness in the

warmed soils (fig. S1B). Furthermore, a PERMANOVA analysis revealed no significant effect of warming on the taxonomic composition of mRNA reads assigned on family level (fig. S2B and table S8), contrasting the observation of a significant effect of warming on the composition of expressed KOs (fig. S2A). Correspondingly, a differential expression analysis of all mRNA reads assigned on family level did not reveal any overall significant differences in the taxonomic composition between ambient and warmed soils (A_T versus E_T; table S19). Repeating the differential expression analysis on subsets representing bacterial families and/or considering only functionally and taxonomically classified reads identified up to three families with differential abundances between A_T and E_T (table S19). However, these taxa accounted for less than 0.05% of the whole communities, affirming that these minor changes in the taxonomic composition were not responsible for the gene expression changes. Furthermore, no significant differences in the community composition of the mRNA read pools between the ambient sites (MTW-A_T versus LTW-A_T) that could potentially explain the lack of taxonomic changes were observed (table S20). In contrast, significant differences between the warmed sites were observed (MTW-E_T versus LTW-E_T; table S20), prompting us to investigate taxonomic composition of mRNA read pools, abundance pattern, and changes in relative abundances of both sites individually (fig. S9). While the taxonomic composition of mRNA reads assigned on family level did not change in response to medium-term warming (MTW-A_T versus MTW-E_T), it did in response to long-term warming (LTW-A_T versus LTW-E_T; table S21). Up to 44 families, five orders, three classes, and six phyla showed a differential abundance between LTW-A_T and LTW-E_T. These taxa accounted for less than 2% of the whole communities (table S21), and up to 75% of the families displaying a differential abundance between LTW-A_T and LTW-E_T represented fungal families with lower relative mRNA read abundance in the warmed soils (table S21). Thus, the earlier-mentioned functional changes observed within the bacterial community in response to warming (Figs. 2 and 3) were not related to a shift in the taxonomic composition (of mRNA reads assigned on family level).

We attempted to increase the taxonomic resolution by assembling the metatranscriptome reads (see the Supplementary Materials). Our approach using rnaSPAdes (29), however, did not provide a sufficient number of long mRNA contigs (<10% of functionally annotated mRNA contigs were longer than the unassembled reads). Also, previous studies using amplicon sequencing of rRNA genes did not indicate warming-induced changes of the microbial community composition at genus and operational taxonomic unit (OTU) level (15, 16, 30). Together, these results provide evidence for a decoupling of microbial community structure and functions, as recently indicated in studies of different ecosystems including short-term warmed peat soil (31–35). While we observed the same central physiological responses in MTW and LTW, only minor taxonomic changes in the community composition were observed and these changes differed between MTW and LTW. In line with this, an extensive screening of all phyla, classes, orders, and families with a mean relative abundance of ≥1‰ in MTW-A_T, MTW-E_T, LTW-A_T, or LTW-E_T revealed that, on average, nearly two-thirds of all taxa (63.7%) showed taxon-specific expression patterns reflecting the overall temperature-dependent expression patterns of central carbohydrate metabolism, energy metabolism, and protein biosynthesis (Fig. 3D and fig. S11). However, the percentage of taxa exhibiting the pattern varied between 43 and 95% depending on the

KEGG3 category and the warming duration and was clearly highest for the KEGG3 categories related to protein biosynthesis and energy metabolism.

Down-regulation of the protein biosynthesis machinery as common physiological response of microorganisms to soil warming?

The down-regulation of the protein biosynthesis machinery, especially of ribosomal proteins, across the bacterial community (Fig. 3D), which notably does not imply a down-regulation of the process (i.e., protein biosynthesis) itself, was the most pronounced response of the microbial communities to soil warming of +6°C (Fig. 2A). Combined with the reduced total RNA content per unit of microbial C in the warmed soils (Fig. 1C), these data suggested that the ribosome content per bacterial cell is lower in the warmed soils than in their ambient counterparts, as rRNA can account for >90% of the total cellular RNA content (36). Besides higher temperatures, the warmed ForHot soils are also characterized by a lower C, N, and P content (16–18), indicating that nutrient limitation may also have contributed to promoting a reduction of bacterial cellular ribosome content. In line with this, starving Escherichia coli and Salmonella spp. cells reduce their ribosomal content (37, 38), suggesting that a down-regulation of the translation machinery is metabolically favorable in nutrient-limited ecosystems (39). Since the translation machinery accounts for up to 40% of total cellular proteins (40) and protein biosynthesis is the costliest type of macromolecular synthesis (41–43), a reduced number of ribosomes would furthermore reduce the energy costs (ATP) related to cell maintenance and replication. The indicated warming-induced down-regulation of membrane-bound energy-harvesting complexes including ATP synthase (Fig. 2B) might therefore be directly linked to the down-regulation of the protein biosynthesis machinery.

The described down-regulation of the protein biosynthesis machinery and energy-harvesting complexes do not necessarily reflect a down-regulation of the processes itself. Protein and ATP synthesis rates (per ribosome and per ATP synthase complex, respectively) are also highly affected by temperature, with higher temperatures resulting in higher rates. This fits to the higher relative expression levels of genes for nucleotide, amino acid, and inorganic phosphate (Pi) supply, to the protein and ATP synthesis machineries (Fig. 2B and fig. S7). Consequently, the warming-induced down-regulation of the protein biosynthesis machinery and energy-harvesting complexes is not contradictory to a warming-induced up-regulation of cell replication and increased biomass-specific growth rates (16).

In the model organism, E. coli accelerated peptide chain elongation rates per ribosome with increasing temperatures were reported decades ago (44). More recently, it has been shown that lowering the peptide chain elongation rates per ribosome results in increased cellular ribosome contents and reduced growth rates (40, 45). This suggests that bacteria exposed to low temperatures can have higher ribosome contents but still lower growth rates than at higher temperatures. A meta-analysis of the chemical composition (C, N, P, protein, and RNA content) of poikilothermic organisms (46) further indicated a temperature-induced shift toward increased RNA contents (which implies increased ribosome contents) in organisms, i.e., plants ($n = 12$), animals ($n = 15$), and bacteria ($n = 8$), exposed to cold temperature. The same pattern was also observed in a more recent study on the phytoplanktonic species Chlamydomonas reinhardtii (47).

Protein biosynthesis is a central cellular process, and the responsible complexes, especially ribosomes, are conserved in all organisms. There is also substantial evidence for the key regulatory role and temperature responsiveness of this machinery across kingdoms (*47*). Thus, our observation of a warming-induced down-regulation of the protein biosynthesis machinery across the soil bacterial community led to the following hypothesis: Reduction of cellular ribosome content is a key response of soil microorganisms exposed to warming, relevant throughout seasons and primarily a direct response to increasing temperatures (Fig. 4A).

To test this hypothesis, we conducted two supplementary experiments. We extracted RNA from soil samples collected from the same A_T and E_T plots of the geothermal soil temperature gradients in a different season (autumn) 4 years later (October 2020) and conducted a short-term warming experiment using LTW-A_T soil sampled at the same time (Fig. 4, B to D). Our rationale for the first test was that an observation of the same pattern of RNA content relative to soil dry weight, at a different time point and season, would support that ribosome reduction is a long-term warming response and was not merely a onetime observation. The rationale for the experiment was that if cellular ribosome reduction is triggered by short-term temperature change, it is a direct temperature response, not only an indirect effect of lower nutrient concentrations in the warmed soils (Fig. 1B).

The in situ RNA content per unit of soil extracted in autumn 2020 reflected the pattern observed in summer 2016, with a lower RNA content in the warmed soils (Fig. 4C). Likewise, we observed a massive reduction to approximately half the RNA content after 1 week of incubation of ambient soils (A_T) at higher temperature (+6°C), remaining at the lower level throughout the experiment (Fig. 4D, upper bar plots). The decrease of RNA content per unit of microbial

C (a proxy for microbial biomass) matched the decrease per gram dry weight soil (Fig. 4D lower bar plots). Thus, our tests confirmed that cellular ribosome reduction is both a fast and long-term response to soil warming.

In contrast to medium- and long-term warming, short-term warming did not result in a reduction of total C, total N, DOC, and total dissolved N (TDN) content relative to the control. TDN declined over 6 weeks of incubation, but that occurred whether the soil was incubated at ambient or elevated temperature (table S24). Nevertheless, the relative effect of environmental variables affected by warming, such as soil temperature and substrate availability (and quality), on metabolic and physiological changes of microbial cells, including changes of cell size and content, still remains to be determined.

In summary, we think that higher biochemical reaction rates, caused by higher temperatures, allow soil bacteria to reduce their cellular ribosome content. However, due to the higher temperatures, cellular protein biosynthesis rates can be maintained or are even accelerated. By investing less energy and matter into ribosomal proteins, the relative abundance of metabolic proteins increases. This increase together with higher temperature leads to higher enzyme activities accelerating overall metabolism and growth. Hence, the tuning of generally highly abundant ribosomal proteins optimizes growth rates by optimizing cellular resource allocation, as proposed previously (*40*).

A smaller protein biosynthesis machinery combined with maintained enzyme rates would intuitively mean that cells could be synthesized at a lower cost, suggesting increased microbial carbon use efficiency. However, this seems not to be the case, as microbial carbon use efficiency remains constant with soil warming (*16*), contrasting
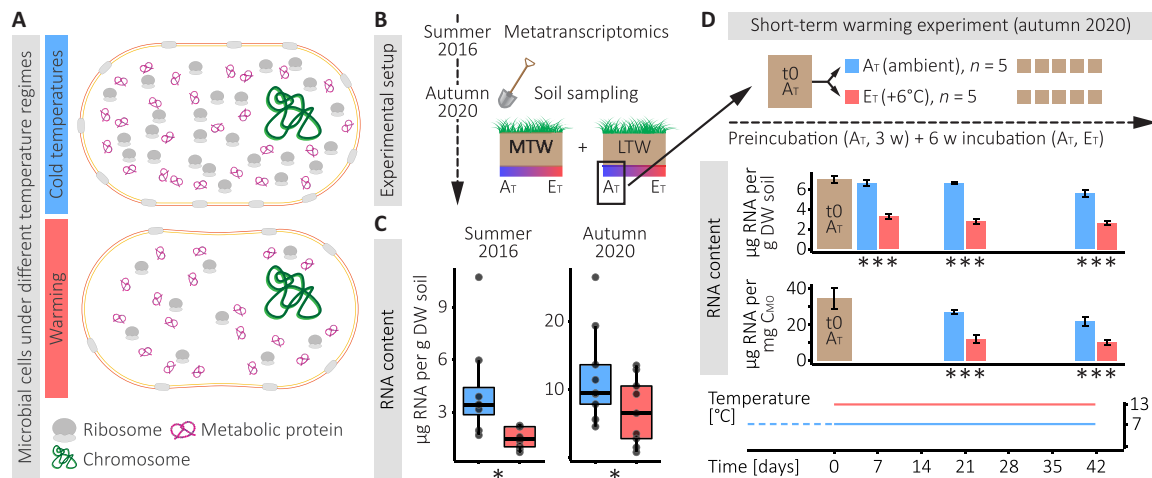
Fig. 4. Hypothesized reduction of cellular ribosome content as response to warming and in situ and experimental indications. (**A**) Schematic representations of microbial cells and cellular constituents under different temperature regimes. The cells vary in the number of ribosomes, ratio between ribosomal and metabolic proteins, amount of membrane-bound complexes, and slightly in size. (**B**) Schematic overview (continuation of Fig. 1A) of the soil sampling conducted in October 2020. The same geothermal soil temperature gradients were samples as in the metatranscriptomics sampling campaign 2016 (see Materials and Methods for more details). (**C**) Comparison of in situ RNA content per gram dry weight (DW) soil between the same plots sampled in two different seasons (summer versus autumn) and 4 years apart (2016 versus 2020). (**D**) Schematic overview and results of a short-term warming experiment conducted with soil sampled from an ambient temperature plot at LTW (see Materials and Methods for more details). After 3 weeks (w) of preincubation of the homogenized soil at ambient temperatures (i.e., mean ambient October soil temperature of 7°C), the first samples (t0, $n = 5$) were taken, and afterward, the soil was distributed to 10 serum bottles. The aerated bottles were incubated for 6 weeks at 7°C (control, $n = 5$) and 13°C (warming treatment, +6°C above ambient, $n = 5$), respectively, and sampled after 1, 3, and 6 weeks of incubation. Line charts depict incubation temperatures, mean total RNA content per gram DW soil, and mean total RNA content per milligram of microbial C (C_{MO}), and error bars represent SD of the mean. For underlying data and details on the statistical analysis presented in (C) and (D), see tables S22 to S24 (*$P < 0.05$; ***$P < 0.001$).

earlier suggestions that warming could lead to less efficient microbial growth (*48*). Although growth efficiency does not increase, a smaller protein biosynthesis machinery may still allow faster cell division, simply because one cell can turn into two within a shorter time if less matter needs to be assimilated, provided the same metabolic rate. In competing with other microorganisms within a system that is becoming depleted of substrates (*16*), this may be a major advantage. Thus, within the boundaries of substrate limitation (*16–18*) and trophic regulation via predators and viruses (*49*), acting together to limit the size of microbial communities, protein biosynthesis regulation may be considered another key mechanism that controls the warming effect on global C cycling.

How warming affects the microbial control of the global C cycle is a key question to better understand soil-climate feedbacks, an answer to which is urgently needed (*4*, *50*). We propose that a down-regulation of the protein biosynthesis machinery is a central physiological response during acclimation of soil bacteria and possibly other environmental microorganisms to short-, medium-, and long-term soil warming. The regulation of protein biosynthesis and the protein biosynthesis machinery allows soil bacteria to maintain high metabolic activities and cell division rates even after decades of warming. This implies that despite reduced soil substrate and nutrient concentrations that follow global (long-term) warming (*4*), soil bacteria will maintain high emissions of CO_2 to the atmosphere.

MATERIALS AND METHODS
Grassland sites and soil sampling
Soil samples were collected from a natural grassland near Hveragerði (64°0′N, 21°11′W), Iceland, in July 2016. The grassland is part of the ForHot experiment (*14*) and features two sites, each consisting of replicated soil temperature gradients (Fig. 1A) that were formed by natural geothermal activity. One site has experienced warming for >50 years, possibly since before 1708 (*14*). Geothermal activities may have varied over time, but warming has been stable in the area since at least 1963, and the warming intensities of the temperature gradients have not varied since detailed measurements began (*14–16*). The second site recently developed similar temperature gradients after an earthquake in 2008. We collected 16 samples that were later analyzed in detail, i.e., four samples of LTW exposed to elevated temperatures (+6°C above ambient, LTW-E_T) and four corresponding controls at ambient temperatures (LTW-A_T) as well as four samples of medium-term (8 years) warmed soils (MTW) exposed to +6°C above ambient temperatures (MTW-E_T) and four corresponding controls (MTW-A_T). The grassland soils are classified as Silandic Andosols, and both sites are dominated by *Agrostis capillaris* with varying undergrowth and vascular plant and moss cover (*14*). We took soil samples (0 to 10 cm depth) from ambient (A_T) and +6°C (E_T) plots of four replicated gradients per site (i.e., eight gradients in total; 4 × LTW and 4 × MTW) at one time point (Fig. 1A and table S1). A_T and E_T plots of each gradient were consecutively sampled. Samples were immediately frozen in liquid N_2 for subsequent nucleic acid extraction and metatranscriptomics after being sieved to 2 mm at site under field conditions.

Physicochemical soil properties
Fresh aliquots of each soil sample were extracted with either 1 M KCl or 0.5 M NaHCO$_3$ solution for 30 min at room temperature or fumigated with chloroform for 48 hours and subsequently extracted using the same extractants. Various soil C and N compounds and soil P compounds (table S1) were quantified in the KCl and NaHCO$_3$ extracts, respectively, using standard procedures (*51*). C_{MO}, N_{MO}, and P_{MO} were calculated as the differences between DOC, TDN, and TDP contents in the fumigated and nonfumigated extracts. Total C and N contents were analyzed in dried soil aliquots using an elemental analyzer coupled to an isotope ratio mass spectrometer (EA-IRMS; EA1110 coupled via a ConFlo III interface to a DeltaPLUS IRMS, Thermo Fisher Scientific). Soil pH was determined from sieved soil samples in 0.05 M CaCl$_2$ solution, and gravimetric water content was determined.

Nucleic acid extractions and sequencing
We extracted total nucleic acids from 16 sieved soil samples (table S4), i.e., four replicates from each of the four sampled soil groups (LTW-A_T, LTW-E_T, MTW-A_T, and MTW-E_T), representing two warming intensities (A_T, +0°C, and E_T, +6°C) of >50-year warmed soils (LTW) and 8-year warmed soils (MTW). These samples were selected because 6°C above ambient is within the predicted and most severe range of (soil) warming over the next 60 to 100 years (*52*, *53*). Each sample was extracted in triplicate (technical replicates), as previously described (*54*). Briefly, a phosphate buffer, a detergent solution containing cetyltrimethylammonium bromide (CTAB), and TE (tris-EDTA)–saturated phenol (pH 8) were added to 0.3 g of soil in a lysis matrix E tube (MP Biomedicals) containing silica beads and shaken vigorously for 30 s (6.5 m s^{-1}) in a FastPrep machine (MP Biomedicals). After centrifugation, the aqueous supernatant was retained. This procedure was repeated two more times using fresh buffer, detergent, and phenol. The three supernatants were then pooled, followed by phenol:chloroform:isoamylalcohol (25:24:1) and chloroform:isoamylalcohol (24:1) extraction and precipitation of the nucleic acids using PEG 8000 (polyethylene glycol, molecular weight 8000). The nucleic acids were treated with deoxyribonuclease (RQ1, Promega) before the metatranscriptomes were generated. DNA (pretreated samples) and RNA quantity and quality were assessed by automated agarose gel electrophoresis (Bioanalyzer 2100, Agilent), a NanoDrop spectrophotometer (ND-1000, Peqlab), and the PicoGreen and RiboGreen assay kits (Thermo Fisher Scientific). RIN (RNA integrity number) ranged from 6.9 to 8.0 (mean RIN: 7.3). Total RNA was amplified using the MessageAmp II-Bacteria Kit (Ambion Life Technologies) with an input of 100 ng of RNA, following the kit protocol, except the RNA was linearly amplified for 14 hours. The kit uses *E. coli* poly(A)-polymerase (while eukaryotic mRNA is naturally polyadenylated, poly-A tailing is necessary to amplify prokaryotic mRNA and pro- and eukaryotic rRNA); it preferentially polyadenylates mRNA and by that facilitates an unbiased amplification and enrichment of total mRNA (*55*). The three technical replicates of each of the 16 samples were pooled before the amplification. Overlapping paired-end 125–base pair reads were sequenced using the HighSeq2500 sequencer (Illumina; library generation: NEBNext Ultra RNA Library Prep Kit for Illumina) at the Vienna Biocenter Core Facilities, Vienna, Austria.

Sequence data preprocessing
We performed the following preprocessing steps and the majority of the subsequent analyses using the Life Science Compute Cluster (LiSC) run by CUBE (Division of Computational Systems Biology), Department of Microbiology and Ecosystem Science, University of Vienna, Austria. PEAR v.0.9.10 (Paired-End reAd mergeR, default

settings) was used to merge the raw paired-end reads (*56*). We subsequently used SortMeRNA v.2.1 to filter out non-rRNA reads from the total RNA reads (*57*). The non-rRNA reads were quality-filtered (-min_len 180 -max_len 240 -min_qual_mean 30 -ns_max_n 5 -trim_tail_right 15 -trim_tail_left 15) using prinseq-lite v.9.20.4 (*58*). A second filtering step was performed to obtain mRNA reads and reduce the size of the dataset for later analyses. All non-rRNA reads that aligned to any sequence in the National Center for Biotechnology Information (NCBI) nr (*59*) database (as of September 2018) using a nonconservative DIAMOND blastx (*60*) search (v.0.9.18, -k 1 -e 0.001) were kept. See table S4 for more details.

Functional and taxonomic annotation

We functionally annotated the total mRNA reads (table S4) by aligning them to the KEGG database (*21*) (as of April 2019) using a DIAMOND blastx (*60*) search (v.0.9.18, -k 1 --min-score 52.5). A prior analysis indicated that a bit score of 52.5 equaled an *e* value of ≤0.0001 [DIAMOND blastx of the same dataset against the KEGG database (*21*) as of February 2019]. We, therefore, used a bit score of 52.5 rather than an *e* value of 0.0001 for all following analyses to obtain a better comparability between different database searches, independent of increasing database sizes. We performed a DIAMOND blastx (*60*) search (v.0.9.25, -k 25 --min-score 52.5) against the NCBI nr (*59*) database (as of October 2019) to obtain taxonomic information for the mRNA reads. We used the program blast2lca, the standalone implementation of the MEGAN (v.6.11.1) LCA (lowest common ancestor)–assignment algorithm, to obtain one taxonomic assignment for each read based on the 25 nr database hits (*61*). The following parameters were used to obtain the LCAs: -ms 50 -me 0.01 -top 5 -mid 0.0 (mapping file: prot_acc2tax-Jul2019X1.abin).

Data and statistical analyses

We used R (*62*) to analyze the data, perform statistical tests, and graphically display the results (Rstudio version 1.1.456) including the R packages ggalluvial version 0.10.0 (https://CRAN.R-project.org/package=ggalluvial), ggplot2 version 3.2.0 (https://CRAN.R-project.org/package=ggplot2), vegan version 2.5-6 (https://CRAN.R-project.org/package=vegan), and edgeR version 3.32.0 (https://bioconductor.org/packages/edgeR). Further details on the R packages can be found in the respective sections. Adobe Illustrator (CC 23.0.2.) was used for final figure editing. Functionally annotated and taxonomically classified mRNA datasets were merged (func.tax.data). Functionally annotated mRNA reads that lacked a taxonomic classification were tagged with "no match." The resulting data were normalized and filtered.

Filtering and normalization

First, we normalized the data to library size and transferred them to per mil (‰). Second, only functions (KOs, i.e., KEGG database entries, i.e., ortholog genes) present in all four replicates of at least one group (LTW-A_T, LTW-E_T, MTW-A_T, or MTW-E_T) were kept (removing 0.6‰ of the data). Third, low abundant functions were removed by filtering out KOs with a total relative abundance (sum of all 16 datasets) <0.1‰ (removing 4.6‰ of the data remaining after the previous step), which equaled a mean relative abundance of a specific function per sample of <0.00625‰ [mean relative abundance (‰) = 0.1‰/16]. A second dataset containing all taxonomically classified mRNA reads (without functional annotation) was likewise normalized and transferred. The taxonomy-only dataset (tax.data) was filtered by removing all families (taxonomic strings from domain to family) that were not present in all replicates of at least one group (LTW-A_T, LTW-E_T, MTW-A_T, or MTW-E_T) (removing 0.07‰ of the data); no second filter was applied. Viral reads were summarized before filtering depending on the subsequent analyses.

Analysis of contextual data

Total, dissolved, and microbial C, N, and P concentrations, nucleic acid concentrations, soil pH, and water content were individually tested for significant differences between defined groups (groups = A_T and E_T, MTW and LTW, MTW-A_T, MTW-E_T, LTW-A_T, and LTW-E_T) using two-way ANOVAs (basic R function aov) and computing Tukey honest significant differences (basic R function TukeyHSD) to evaluate sample selection and grouping. X-fold changes were calculated in R: (mean E_T/mean A_T).

Boxplots

Boxplots were generated using geom_boxplot (R package ggplot2).

Correlations

The basic R function cor.test was used to identify associations between microbial biomass (using microbial C as proxy) and nucleic acid contents by applying Spearman's rank correlation (two-sided; *P* values were corrected for multiple testing using Benjamini-Hochberg procedure, basic R function p.adjust). The ggplot function geom_smooth was used to indicate correlations (method = lm).

Richness estimates

Taxonomic (family) and functional (KO) richness was estimated from raw read counts [families and KOs not present in all four replicates of at least one group (LTW-A_T, LTW-E_T, MTW-A_T, or MTW-E_T) were considered as noise and excluded] using the vegan function rarefy. The basic R function t.test was used to perform two-sided Student's *t* tests to identify significant differences between A_T and E_T (of LTW and MTW, respectively, or across LTW and MTW). Obtained *P* values were corrected for multiple testing (Benjamini-Hochberg procedure, basic R function p.adjust).

NMDS and PERMANOVA

Nonmetric multidimensional scaling (NMDS) was used to obtain ordination plots depicting (dis)similarities between expressed microbial functions (KOs) and microbial community structures of the samples (fig. S2). We used the metaMDS function implemented in the R package vegan, two dimensions, and a maximum of 10,000 random starts in search of a stable solution. The sequencing data were normalized and filtered as described above before the NMDS analyses. GUSTA ME (GUide to STatistical Analysis in Microbial Ecology) (*63*) was consulted for selecting the appropriate dissimilarity index (i.e., "canberra"). PERMANOVA (vegan function adonis) was used to identify the effect of warming (A_T and E_T) and warming duration (LTW and MTW), respectively, on the distribution of samples by gene expression (9,999 permutations, dissimilarity index "canberra").

Alluvial plots

Alluvial plots (Sankey diagrams) were created using the R package ggalluvial. Individual Sankey diagrams were manually merged if more than two levels were shown.

Heatmaps

Heatmaps were generated using the geom_tile function of the ggplot2 R package. Before plotting, normalized data were transformed by *z* scoring, either over all 16 samples or separately for LTW and MTW. Two explorative abundance pattern filters were subsequently applied for selecting patterns of interest. Abundance pattern filter applied on KEGG3 categories (figs. S6 and S7): The relative abundances of KEGG3 categories between A_T and E_T across all samples were

compared. Patterns were retained only if (i) at least six samples of one temperature group (A_T or E_T) were higher than the third highest sample of the other temperature group (E_T or A_T) and at least seven samples of one temperature group (E_T or A_T) were lower than the third lowest sample of the other temperature group (A_T or E_T) or (ii) at least seven samples of one temperature group (A_T or E_T) were higher than the third highest sample of the other temperature group (E_T or A_T) and at least six samples of one temperature group (E_T or A_T) were lower than the third lowest sample of the other temperature group (A_T or E_T). Therefore, the critical threshold to pass the abundance pattern filter lies at 80% consensus with the most stringent warming-associated distribution (i.e., the eight highest relative transcript abundances are found in one temperature group and the eight lowest in the opposite temperature group). Abundance pattern filter applied on individual subsets (MTW and LTW): A more stringent filter (referred to as 4/4-filter) was used to analyze the MTW and LTW individually (fig. S9); only taxa with higher or lower relative abundances in all four replicates of one group relative to their counterparts passed the filter threshold (e.g., a taxon passes the filter if the four highest values are found in LTW-A_T and the four lowest in LTW-E_T). Log$_2$-fold changes in mRNA abundances of selected taxonomic groups were calculated in R: log$_2$(mean E_T/mean A_T).

Differential gene expression

To identify differences in gene expression (mRNA abundances) between A_T and E_T (of LTW and MTW, respectively, or across LTW and MTW), DGE analyses were performed using edgeR (function glmQLFTest), recommended for a small number of replicates (<12) (*64*). Raw read counts were filtered as described in the "Filtering and normalization" section but normalized using the default trimmed mean of M-value normalization (TMM) method implemented in edgeR. DGE analysis on functionally annotated mRNA reads (KO level, i.e., orthologous genes) was performed as follows: Eukaryotic mRNA was excluded from the analysis (to eliminate potential biases related to taxonomic composition), and a minimum of 500 physical read counts per sample was used as a threshold for a KO to be considered in the DGE analysis (to exclude infrequent transcripts and allow a taxon-specific breakdown). KOs with an FDR between 0.05 and 0.1 were considered as transcripts of interest when being part of pathways or complexes containing significantly differentially expressed transcripts (FDR < 0.05). DGE analysis on taxonomically annotated mRNA reads (domain/kingdom, phylum, class, order, and family level): DGE analyses were performed on taxonomically annotated datasets (func.tax.data and tax.data). The threshold for a taxon to be considered in the DGE analysis varied depending on the taxonomic rank and ranged from 5 to 500 physical mRNA reads.

Supplementary experiments
RNA extractions

The same A_T and E_T plots that were analyzed in detail in our metatranscriptomics study were resampled in October 2020, 4 years after the metatranscriptomics sampling campaign (Fig. 4B and table S22). After removing the plant cover, soil from the upper 5 cm was sampled and kept on dry ice or at −80°C until processing. The samples were homogenized and grinded on liquid N. Afterward, total nucleic acids were extracted as described above. Total RNA content was quantified using the Qubit RNA HS Assay Kit (Thermo Fisher Scientific). The basic R function t.test was used to perform a one-sided Student's *t* test to test the hypothesis that warming leads to a reduction in the RNA content.

Short-term warming experiment

A short-term warming experiment (Fig. 4D) was performed using LTW-A_T soil sampled in October 2020. The sample (~270 g) was shipped (on cool packs), sieved (2 mm), homogenized, and preincubated (3 weeks) in a glass beaker (in the dark, tightly closed with tin foil) at the mean ambient October soil temperature (7°C). After preincubation, the homogenized soil was sampled (t0 sampling; starting point of the experiment; *n* = 5). Subsequently, the remaining soil was distributed to 10 serum bottles (closed with a rubber stopper). The regularly aerated bottles were incubated for 6 weeks at 7°C (control, *n* = 5) and 13°C (warming treatment, +6°C above ambient, *n* = 5), respectively, and sampled after 1, 3, and 6 weeks of incubation. Total nucleic acids were extracted using the phenol:chloroform triple bead-beating protocol described above. Total RNA content was quantified using the Qubit RNA HS Assay Kit (Thermo Fisher Scientific). Microbial C and total soil C and N were determined as described above. The basic R function t.test was used to perform two-sided Student's *t* tests to identify significant differences between control and warming treatment at the different sampling time points.

REFERENCES AND NOTES

1. IPCC, Special Report: Global Warming of 1.5 °C; www.ipcc.ch/sr15/.
2. IPCC, *Contribution of Working Group I to the Fifth Assessment Report of the Intergovernmental Panel on Climate Change* (Cambridge Univ. Press, 2013).
3. J. G. Canadell, C. Le Quéré, M. R. Raupach, C. B. Field, E. T. Buitenhuis, P. Ciais, T. J. Conway, N. P. Gillett, R. A. Houghton, G. Marland, Contributions to accelerating atmospheric CO2 growth from economic activity, carbon intensity, and efficiency of natural sinks. *Proc. Natl. Acad. Sci. U.S.A.* **104**, 18866–18870 (2007).
4. J. K. Jansson, K. S. Hofmockel, Soil microbiomes and climate change. *Nat. Rev. Microbiol.* **18**, 35–46 (2020).
5. C. M. Kallenbach, S. D. Frey, A. S. Grandy, Direct evidence for microbial-derived soil organic matter formation and its ecophysiological controls. *Nat. Commun.* **7**, 13630 (2016).
6. C. Liang, W. Amelung, J. Lehmann, M. Kästner, Quantitative assessment of microbial necromass contribution to soil organic matter. *Glob. Chang. Biol.* **25**, 3578–3590 (2019).
7. K. Wang, C. Peng, Q. Zhu, X. Zhou, M. Wang, K. Zhang, G. Wang, Modeling global soil carbon and soil microbial carbon by integrating microbial processes into the ecosystem process model TRIPLEX-GHG. *J. Adv. Model. Earth Syst.* **9**, 2368–2384 (2017).
8. J. M. Melillo, S. D. Frey, K. M. DeAngelis, W. J. Werner, M. J. Bernard, F. P. Bowles, G. Pold, M. A. Knorr, A. S. Grandy, Long-term pattern and magnitude of soil carbon feedback to the climate system in a warming world. *Science* **358**, 101–105 (2017).
9. A. L. Romero-Olivares, S. D. Allison, K. K. Treseder, Soil microbes and their response to experimental warming over time: A meta-analysis of field studies. *Soil Biol. Biochem.* **107**, 32–40 (2017).
10. W. Knorr, I. C. Prentice, J. I. House, E. A. Holland, Long-term sensitivity of soil carbon turnover to warming. *Nature* **433**, 298–301 (2005).
11. J. C. Carey, J. Tang, P. H. Templer, K. D. Kroeger, T. W. Crowther, A. J. Burton, J. S. Dukes, B. Emmett, S. D. Frey, M. A. Heskel, L. Jiang, M. B. Machmuller, J. Mohan, A. M. Panetta, P. B. Reich, S. Reinsch, X. Wang, S. D. Allison, C. Bamminger, S. Bridgham, S. L. Collins, G. De Dato, W. C. Eddy, B. J. Enquist, M. Estiarte, J. Harte, A. Henderson, B. R. Johnson, K. S. Larsen, Y. Luo, S. Marhan, J. M. Melillo, J. Peñuelas, L. Pfeifer-Meister, C. Poll, E. Rastetter, A. B. Reinmann, L. L. Reynolds, I. K. Schmidt, G. R. Shaver, A. L. Strong, V. Suseela, A. Tietema, Temperature response of soil respiration largely unaltered with experimental warming. *Proc. Natl. Acad. Sci. U.S.A.* **113**, 13797–13802 (2016).
12. M. A. Bradford, C. A. Davies, S. D. Frey, T. R. Maddox, J. M. Melillo, J. E. Mohan, J. F. Reynolds, K. K. Treseder, M. D. Wallenstein, Thermal adaptation of soil microbial respiration to elevated temperature. *Ecol. Lett.* **11**, 1316–1327 (2008).
13. M. U. F. Kirschbaum, Soil respiration under prolonged soil warming: Are rate reductions caused by acclimation or substrate loss? *Glob. Chang. Biol.* **10**, 1870–1877 (2004).
14. B. D. Sigurdsson, N. I. W. Leblans, S. Dauwe, E. Gudmundsdóttir, P. Gundersen, G. E. Gunnarsdóttir, M. Holmstrup, K. Ilieva-Makulec, T. Kätterer, B. Marteinsdóttir, M. Maljanen, E. S. Oddsdóttir, I. Ostonen, J. Peñuelas, C. Poeplau, A. Richter, P. Sigurdsson,

P. Van Bodegom, H. Wallander, J. Weedon, I. Janssens, Geothermal ecosystems as natural climate change experiments: The ForHot research site in Iceland as a case study. *Icel. Agric. Sci.* **29**, 53–71 (2016).

15. T. W. N. Walker, I. A. Janssens, J. T. Weedon, B. D. Sigurdsson, A. Richter, J. Peñuelas, N. I. W. Leblans, M. Bahn, M. Bartrons, C. De Jonge, L. Fuchslueger, A. Gargallo-Garriga, G. E. Gunnarsdóttir, S. Marañón-Jiménez, E. S. Oddsdóttir, I. Ostonen, C. Poeplau, J. Prommer, D. Radujković, J. Sardans, P. Sigurðsson, J. L. Soong, S. Vicca, H. Wallander, K. Ilieva-Makulec, E. Verbruggen, A systemic overreaction to years versus decades of warming in a subarctic grassland ecosystem. *Nat. Ecol. Evol.* **4**, 101–108 (2020).

16. T. W. N. Walker, C. Kaiser, F. Strasser, C. W. Herbold, N. I. W. Leblans, D. Woebken, I. A. Janssens, B. D. Sigurdsson, A. Richter, Microbial temperature sensitivity and biomass change explain soil carbon loss with warming. *Nat. Clim. Chang.* **8**, 885–889 (2018).

17. S. Marañón-Jiménez, J. L. Soong, N. I. W. Leblans, B. D. Sigurdsson, J. Peñuelas, A. Richter, D. Asensio, E. Fransen, I. A. Janssens, Geothermally warmed soils reveal persistent increases in the respiratory costs of soil microbes contributing to substantial C losses. *Biogeochemistry* **138**, 245–260 (2018).

18. S. Marañón-Jiménez, J. Peñuelas, A. Richter, B. D. Sigurdsson, L. Fuchslueger, N. I. W. Leblans, I. A. Janssens, Coupled carbon and nitrogen losses in response to seven years of chronic warming in subarctic soils. *Soil Biol. Biochem.* **134**, 152–161 (2019).

19. C. Poeplau, T. Kätterer, N. I. W. Leblans, B. D. Sigurdsson, Sensitivity of soil carbon fractions and their specific stabilization mechanisms to extreme soil warming in a subarctic grassland. *Glob. Chang. Biol.* **23**, 1316–1327 (2017).

20. T. Urich, A. Lanzén, J. Qi, D. H. Huson, C. Schleper, S. C. Schuster, Simultaneous assessment of soil microbial community structure and function through analysis of the meta-transcriptome. *PLOS ONE* **3**, e2527 (2008).

21. M. Kanehisa, S. Goto, KEGG: Kyoto Encyclopedia of Genes and Genomes. *Nucleic Acids Res.* **28**, 27–30 (2000).

22. H. L. Burgos, K. O'Connor, P. Sanchez-Vazquez, R. L. Gourse, Roles of transcriptional and translational control mechanisms in regulation of ribosomal protein synthesis in *Escherichia coli*. *J. Bacteriol.* **199**, e00407-17 (2017).

23. P. Jurtshuk, Bacterial metabolism, in *Medical Microbiology*, S. Baron Ed. (University of Texas Medical Branch at Galveston, Texas, ed. 4, 1996), chap. 4.

24. P. Roy Chowdhury, S. M. Golas, L. V. Alteio, J. T. E. Stevens, A. F. Billings, J. L. Blanchard, J. M. Melillo, K. M. DeAngelis, The transcriptional response of soil bacteria to long-term warming and short-term seasonal fluctuations in a terrestrial forest. *Front. Microbiol.* **12**, 666558 (2021).

25. L. I. Rothfield, S. S. Justice, Bacterial cell division: The cycle of the ring. *Cell* **88**, 581–584 (1997).

26. J. Männik, B. E. Walker, J. Männik, Cell cycle-dependent regulation of FtsZ in Escherichia coli in slow growth conditions. *Mol. Microbiol.* **110**, 1030–1044 (2018).

27. J. D. Wang, P. A. Levin, Metabolism, cell growth and the bacterial cell cycle. *Nat. Rev. Microbiol.* **7**, 822–827 (2009).

28. P. Carini, P. J. Marsden, J. W. Leff, E. E. Morgan, M. S. Strickland, N. Fierer, Relic DNA is abundant in soil and obscures estimates of soil microbial diversity. *Nat. Microbiol.* **2**, 16242 (2016).

29. E. Bushmanova, D. Antipov, A. Lapidus, A. D. Prjibelski, RnaSPAdes: A de novo transcriptome assembler and its application to RNA-Seq data. *Gigascience* **8**, giz100 (2019).

30. D. Radujković, E. Verbruggen, B. D. Sigurdsson, N. I. W. Leblans, I. A. Janssens, S. Vicca, J. T. Weedon, Prolonged exposure does not increase soil microbial community compositional response to warming along geothermal gradients. *FEMS Microbiol. Ecol.* **94**, fix174 (2018).

31. A. Frossard, L. Gerull, M. Mutz, M. O. Gessner, Disconnect of microbial structure and function: Enzyme activities and bacterial communities in nascent stream corridors. *ISME J.* **6**, 680–691 (2012).

32. W. Purahong, M. Schloter, M. J. Pecyna, D. Kapturska, V. Däumlich, S. Mital, F. Buscot, M. Hofrichter, J. L. M. Gutknecht, D. Krüger, Uncoupling of microbial community structure and function in decomposing litter across beech forest ecosystems in Central Europe. *Sci. Rep.* **4**, 7014 (2014).

33. A. Söllinger, A. T. Tveit, M. Poulsen, S. J. Noel, M. Bengtsson, J. Bernhardt, A. L. Frydendahl Hellwing, P. Lund, K. Riedel, C. Schleper, O. Højberg, T. Urich, Holistic assessment of rumen microbiome dynamics through quantitative metatranscriptomics reveals multifunctional redundancy during key steps of anaerobic feed degradation. *mSystems* **3**, e00038-18 (2018).

34. K. Min, K. Buckeridge, S. E. Ziegler, K. A. Edwards, S. Bagchi, S. A. Billings, Temperature sensitivity of biomass-specific microbial exo-enzyme activities and CO_2 efflux is resistant to change across short- and long-term timescales. *Glob. Chang. Biol.* **25**, 1793–1807 (2019).

35. S. Yang, S. Liebner, M. M. Svenning, A. T. Tveit, Decoupling of microbial community dynamics and functions in Arctic peat soil exposed to short term warming. *Mol. Ecol.* **30**, 5094–5104 (2021).

36. S. J. Blazewicz, R. L. Barnard, R. A. Daly, M. K. Firestone, Evaluating rRNA as an indicator of microbial activity in environmental communities: Limitations and uses. *ISME J.* **7**, 2061–2068 (2013).

37. B. D. Davis, S. M. Luger, P. C. Tai, Role of ribosome degradation in the death of starved Escherichia coli cells. *J. Bacteriol.* **166**, 439–445 (1986).

38. D. Hsu, L. M. Shih, Y. C. Zee, Degradation of rRNA in Salmonella strains: A novel mechanism to regulate the concentrations of rRNA and ribosomes. *J. Bacteriol.* **176**, 4761–4765 (1994).

39. J. A. Klappenbach, J. M. Dunbar, T. M. Schmidt, rRNA operon copy number reflects ecological strategies of bacteria. *Appl. Environ. Microbiol.* **66**, 1328–1333 (2000).

40. E. Bosdriesz, D. Molenaar, B. Teusink, F. J. Bruggeman, How fast-growing bacteria robustly tune their ribosome concentration to approximate growth-rate maximization. *FEBS J.* **282**, 2029–2044 (2015).

41. A. H. Stouthamer, A theoretical study on the amount of ATP required for synthesis of microbial cell material. *Antonie Van Leeuwenhoek* **39**, 545–565 (1973).

42. J. B. Russell, The energy spilling reactions of bacteria and other organisms. *J. Mol. Microbiol. Biotechnol.* **13**, 1–11 (2007).

43. F. Buttgereit, M. D. Brand, A hierarchy of ATP-consuming processes in mammalian cells. *Biochem. J.* **312**, 163–167 (1995).

44. J. Ryals, R. Little, H. Bremer, Temperature dependence of RNA synthesis parameters in Escherichia coli. *J. Bacteriol.* **151**, 879–887 (1982).

45. M. Scott, C. W. Gunderson, E. M. Mateescu, Z. Zhang, T. Hwa, Interdependence of cell growth and gene expression: Origins and consequences. *Science* **330**, 1099–1102 (2010).

46. H. A. Woods, W. Makino, J. B. Cotner, S. E. Hobbie, J. F. Harrison, K. Acharya, J. J. Elser, Temperature and the chemical composition of poikilothermic organisms. *Funct. Ecol.* **17**, 237–245 (2003).

47. D. O. Hessen, O. T. Hafslund, T. Andersen, C. Broch, N. K. Shala, M. W. Wojewodzic, Changes in stoichiometry, cellular RNA, and alkaline phosphatase activity of *Chlamydomonas* in response to temperature and nutrients. *Front. Microbiol.* **8**, 18 (2017).

48. W. R. Wieder, G. B. Bonan, S. D. Allison, Global soil carbon projections are improved by modelling microbial processes. *Nat. Clim. Chang.* **3**, 909–912 (2013).

49. M. P. Thakur, S. Geisen, Trophic regulations of the soil microbiome. *Trends Microbiol.* **9**, 771–780 (2019).

50. R. D. Bardgett, C. Freeman, N. J. Ostle, Microbial contributions to climate change through carbon cycle feedbacks. *ISME J.* **2**, 805–814 (2008).

51. R. Hood-Nowotny, N. H.-N. Umana, E. Inselbacher, P. Oswald-Lachouani, W. Wanek, Alternative methods for measuring inorganic, organic, and total dissolved nitrogen in soil. *Soil Sci. Soc. Am. J.* **74**, 1018–1027 (2010).

52. M. S. Torn, A. Chabbi, P. Crill, P. J. Hanson, I. A. Janssens, Y. Luo, C. H. Pries, C. Rumpel, M. W. I. Schmidt, J. Six, M. Schrumpf, B. Zhu, A call for international soil experiment networks for studying, predicting, and managing global change impacts. *SOIL Discuss.* **2**, 133–151 (2015).

53. IPCC, Special report: Climate Change and Land, www.ipcc.ch/srccl/.

54. R. Angel, P. Claus, R. Conrad, Methanogenic archaea are globally ubiquitous in aerated soils and become active under wet anoxic conditions. *ISME J.* **6**, 847–862 (2012).

55. J. Frias-Lopez, Y. Shi, G. W. Tyson, M. L. Coleman, S. C. Schuster, S. W. Chisholm, E. F. DeLong, Microbial community gene expression in ocean surface waters. *Proc. Natl. Acad. Sci. U.S.A.* **105**, 3805–3810 (2008).

56. J. Zhang, K. Kobert, T. Flouri, A. Stamatakis, PEAR: A fast and accurate Illumina paired-end reAd mergeR. *Bioinformatics* **30**, 614–620 (2014).

57. E. Kopylova, L. Noé, H. Touzet, SortMeRNA: Fast and accurate filtering of ribosomal RNAs in metatranscriptomic data. *Bioinformatics* **28**, 3211–3217 (2012).

58. R. Schmieder, R. Edwards, Quality control and preprocessing of metagenomic datasets. *Bioinformatics* **27**, 863–864 (2011).

59. NCBI Resource Coordinators, Database resources of the National Center for Biotechnology Information. *Nucleic Acids Res.* **46**, D8–D13 (2018).

60. B. Buchfink, C. Xie, D. H. Huson, Fast and sensitive protein alignment using DIAMOND. *Nat. Methods* **12**, 59–60 (2015).

61. D. H. Huson, S. Beier, I. Flade, A. Górska, M. El-Hadidi, S. Mitra, H. J. Ruscheweyh, R. Tappu, MEGAN community edition—Interactive exploration and analysis of large-scale microbiome sequencing data. *PLOS Comput. Biol.* **12**, e1004957 (2016).

62. R Core Development Team, R: A Language and Environment for Statistical Computing (R Foundation Statistical Computing); www.r-project.org/.

63. P. L. Buttigieg, A. Ramette, A guide to statistical analysis in microbial ecology: A community-focused, living review of multivariate data analyses. *FEMS Microbiol. Ecol.* **90**, 543–550 (2014).

64. N. J. Schurch, P. Schofield, M. Gierliński, C. Cole, A. Sherstnev, V. Singh, N. Wrobel, K. Gharbi, G. G. Simpson, T. Owen-Hughes, M. Blaxter, G. J. Barton, How many biological replicates are needed in an RNA-seq experiment and which differential expression tool should you use? *RNA* **22**, 839–851 (2016).

65. S. Nurk, A. Bankevich, D. Antipov, A. A. Gurevich, A. Korobeynikov, A. Lapidus, A. D. Prjibelski, A. Pyshkin, A. Sirotkin, Y. Sirotkin, R. Stepanauskas, S. R. Clingenpeel, T. Woyke, J. S. McLean, R. Lasken, G. Tesler, M. A. Alekseyev, P. A. Pevzner, Assembling single-cell genomes and mini-metagenomes from chimeric MDA products. *J. Comput. Biol.* **20**, 714–737 (2013).

66. B. Bushnell, J. Rood, E. Singer, BBMerge—Accurate paired shotgun read merging via overlap. *PLOS ONE* **12**, e0185056 (2017).

ScienceAdvances

Down-regulation of the bacterial protein biosynthesis machinery in response to weeks, years, and decades of soil warming

Andrea SöllingerJoana SénecaMathilde Borg DahlLiabo L. MotlelengJudith PrommerErik VerbruggenBjarni D. SigurdssonIvan JanssensJosep PeñuelasTim UrichAndreas RichterAlexander T. Tveit

View the article online
https://www.science.org/doi/10.1126/sciadv.abm3230
Permissions
https://www.science.org/help/reprints-and-permissions

Use of this article is subject to the Terms of service